

Shubnikov-de Haas measurements on *n*- and *p*-type HgTe-CdTe superlattices^{a)}

D. G. Seiler^{b)}

National Institute of Standards and Technology, Semiconductor Electronics Division, Gaithersburg, Maryland 20899

G. B. Ward and R. J. Justice

Department of Physics, University of North Texas, Denton, Texas 76203

R. J. Koestner, M. W. Goodwin, and M. A. Kinch

Central Research Laboratories, Texas Instruments, Dallas, Texas 75265

J. R. Meyer

Naval Research Laboratory, Washington, DC 20375

(Received 21 November 1988; accepted for publication 8 March 1989)

Oscillatory magnetoresistance (Shubnikov-de Haas) measurements have been used to determine free-carrier effective masses in HgTe-CdTe superlattices. Measurements on an *n*-type superlattice yield an electron mass that is in excellent agreement with theoretical results from a tight-binding band-structure calculation. The *p*-type data are more complex, showing evidence for a light-hole mass at low magnetic fields and a much heavier mass at fields above 2.0 T. This finding is also in agreement with the predictions of band-structure theory.

INTRODUCTION

New artificially structured II-VI narrow gap materials, created by molecular-beam epitaxy (MBE) technology, are characterized by their small effective masses and energy gaps, as well as their nonparabolic energy bands. Systems such as HgTe-CdTe superlattices are of great practical interest because of the ability to separately "tune" both the band gap and the effective mass to desired values for use in applications such as infrared detectors. Infrared absorption spectra¹ and temperature-dependent intrinsic carrier densities from Hall measurements²⁻⁴ have been used to estimate values for the energy gap. However, different measurements must be made in order to extract effective masses, and these have proven more difficult to carry out. In the past, extensive studies on a wide variety of semiconductors have shown that the Shubnikov-de Haas (SdH) effect can be used as a valuable characterization tool for determining effective mass values.⁵ Here we use the SdH effect to determine effective masses in both *n*- and *p*-type HgTe-CdTe II-VI superlattice materials.

In spite of the valuable information about material properties that can be obtained from SdH studies, very little work has been carried out on HgTe-CdTe superlattices. In part this is due to the increased difficulty of growth for Hg-based systems compared to the III-V materials. Only two previous studies on *p*-type samples^{2,6} and two on *n*-type samples^{7,8} have been reported in the literature. In this paper, we report on the observation and investigation of SdH oscillations in both *n*- and *p*-type HgTe-CdTe superlattices. Furthermore, we have carried out a new and more extensive study of *p*-type superlattices. Our data and analysis suggest a possible resolution to the apparent contradiction between previous SdH results reported by Woo and co-workers⁶ and those of Goodwin *et al.*² for *p*-type material.

Ong *et al.*⁷ observed SdH oscillations and the quantized Hall effect in high-mobility *n*-type samples of HgTe-CdTe superlattices grown by a laser-assisted molecular-beam epitaxy method. The samples had thicknesses of 90 Å for the HgTe layers and 40 Å for the CdTe. SdH oscillations could only be seen at high fields (> 2 T). They found indications of two different electrons, one with $m^* = 0.025m_0$ and the other with one half this value. Further SdH studies on these same samples were very recently carried out by Ghenim *et al.*⁸ using a first derivative field modulation technique to enhance the SdH data. Their results indicated that three subbands in the quantum well contribute to the conductivity and that the intermediate SdH component has an electron effective mass five times larger than the mass of the lower-frequency SdH component. These results demonstrate that the SdH effect can provide valuable information needed to unravel the complexities of the HgTe-CdTe band structure.

EXPERIMENTAL WORK

HgTe-CdTe superlattices were grown on (112) CdTe substrates with CdTe buffer layers with a Riber 2300 molecular-beam epitaxy (MBE) machine. Bond pads were made by evaporating Pb/In onto the sides of the delineated structures to assure contacting to all the layers. Temperature-dependent Hall measurements and variable field magnetoconductivity measurements established the *n*- or *p*-type nature of the samples.

Measurements of the SdH oscillations were enhanced by using ac magnetic field modulation and lock-in amplifier techniques for fields up to 12 T. A Bessel function then modulates the usual SdH amplitude, reducing the oscillatory signal amplitude at high magnetic fields. Detection of the second harmonic by the lock-in produces an output that is similar to the second derivative of the dc SdH oscillations. Spin splitting is often observed in SdH oscillatory structure; higher harmonics are then necessary to take this into account. The resulting SdH expression becomes

^{a)} All experimental work carried out at the University of North Texas.

^{b)} Formerly at the University of North Texas.

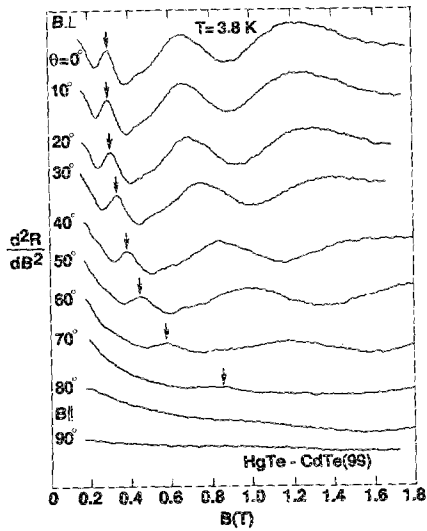


FIG. 1. Angular dependence of the SdH oscillations for *p*-type sample No. 99 showing a $\cos \theta$ shift of the extrema that is typical of 2D behavior.

$$\frac{\Delta \rho}{\rho_0} \approx \sum_{S=1}^m \sum_{R=1}^{\infty} 2A_{TS}^{(R)}(B) \cos\left(\frac{2\pi R}{P_S B} + \phi_S\right) J_2(R\sigma_S), \quad (1)$$

where $\sigma_S = 2\pi B_M / P_S B^2$, and B_M is the amplitude of the small ac magnetic field. P_S is the SdH period and ϕ_S is the phase factor for the S th carrier component, and

$$A_{TS}^{(R)}(B) = \frac{5\sqrt{2}}{2} \pi^2 R^{1/2} (-1)^R \frac{k_B T}{B^{1/2}} \left(\frac{m_S^* c}{E_F e \hbar}\right)^{1/2} \times \frac{e^{-R\beta T_{D_S} m_S^*/B} \cos(R\pi m_S^* g_S/2)}{\sinh(R\beta T_{D_S} m_S^*/B)}, \quad (2)$$

where T_{D_S} is the Dingle temperature, g_S is the g factor, and $m_S^* = m_S^*/m_0$ is the reduced effective mass for the S th component. $\beta = 2\pi k_B m_0 c / e \hbar = 1.468 \times 10^5 \text{ G/K}$. Generally, only harmonics to order $R = 3$ are necessary for Eq. (1) to adequately describe SdH data outside the extreme quantum limit region.

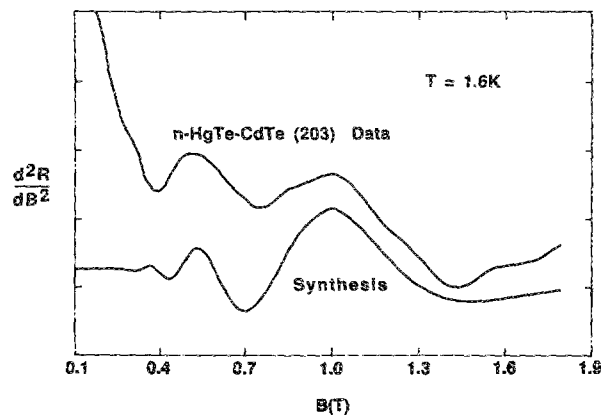


FIG. 2. SdH oscillatory data measured on *n*-type sample No. 203 along with a theoretical synthesis using Eqs. (1) and (2) with the inclusion of three harmonic terms. Except for the large monotonic background present in the experimental data at low fields, there is good agreement.

RESULTS AND DISCUSSION

Results of SdH studies on several *n*- and *p*-type superlattices are summarized in Table I, along with sample growth details. For the three samples in which SdH oscillations were observed, the shifts of the extrema versus magnetic field orientation were found to have the $\cos \theta$ dependence that is typical of 2D behavior. This is illustrated in Fig. 1, which shows the SdH oscillations (second derivative of the oscillatory magnetoresistance obtained from the output of a lock-in amplifier) for sample No. 99 as the magnetic field is rotated from the superlattice growth direction ($\theta = 0^\circ$) to the in-plane orientation (90°).

The SdH oscillatory data at $T = 1.6 \text{ K}$ for an *n*-type superlattice No. 203 are shown in Fig. 2. The electron effective mass may be derived from the temperature dependence of the SdH amplitude, which is given in Fig. 3. Here we have plotted the ratio of the amplitudes for various temperatures and fit the usual simple theoretical variation

$$T \sinh(\beta T_0 m^*/m_0 B) / T_0 \sinh(\beta T m^*/m_0 B)$$

to the data by choosing m^* to give the best fit. As indicated by the curve in Fig. 3, the data are well described by this expression if one uses $m^* = 0.021 \pm 0.004 m_0$. Values for T_D and the g factor can be obtained by synthesizing the oscillatory data shown in Fig. 2 using T_D and g as adjustable parameters. The synthesis shown in Fig. 2 is seen to be in reasonable agreement with the data for $T_D = 11 \text{ K}$, $g = 30$, and $\phi = -\pi/4$.

This experimental result may be compared with theoretical dispersion relations obtained using the tight-binding superlattice band-structure formalism of Schulman and Chang.⁹ The HgTe wells of sample No. 203 are too thick (200 Å) for a finite band gap to be opened due to quantum confinement. In the band structure calculated for the appropriate well and barrier thicknesses,¹⁰ the conduction-band minimum is at the Γ point, while the valence band maximum is slightly off center at a finite in-plane wave vector (k_x).

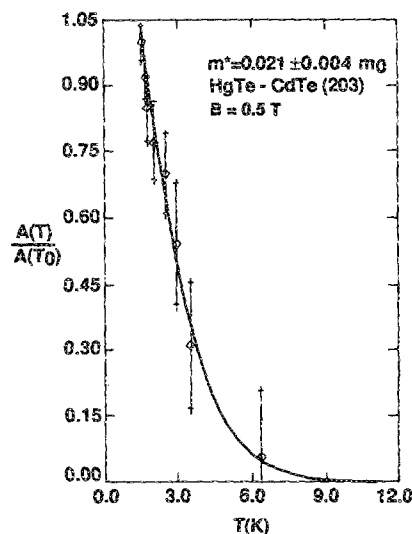


FIG. 3. Normalized SdH amplitudes as a function of temperature for sample No. 203. The solid line shows the theoretical variation predicted from Eq. (2) using only the first harmonic SdH term with $m^* = 0.021 m_0$.

The energy overlap of the two bands is only 0.2 meV, and both bands have very little dispersion in the growth direction (k_z). Since the conduction-band minimum extends along the entire k_z axis, the electrons populate states with all k_z even at low temperatures. The calculated dispersion relations imply an in-plane electron mass of $0.024m_0$ at the zone center ($k_z = 0$) and $0.018m_0$ at the zone boundary ($k_z = \pi/d$, where d is the superlattice period). This "broadening" of the electron mass is mild enough that to first order, conventional SdH analysis should still apply. If we average the two external values for the electron mass, we get a theoretical result that agrees almost exactly with the experimental determination.

The most extensive experimental results were obtained for p -type sample No. 99. The temperature dependence of the SdH oscillations for this sample are shown in Fig. 4. The figure illustrates that for $T > 15$ K, the oscillations are almost completely damped out at these low magnetic fields. This is also illustrated in Fig. 5, which plots the temperature dependence of the low magnetic field oscillation amplitudes. Using the analysis discussed above for electrons, the fit to the data implies $m^* = 0.012 \pm 0.001m_0$. This indicates that at low fields (0–2 T), light-mass carriers dominate the transport.

We were able to extend these SdH measurements up to much higher fields with the recent installation of a superconducting magnet at the University of North Texas. This has permitted the observation of a more complex behavior in the SdH oscillatory data as shown in Fig. 6. The data seem to imply that there are two different sets of holes involved in the transport processes, one dominating at low fields and the other at high fields. Consequently, a two component synthesis ($S = 1, 2$) was done using Eqs. (1) and (2) with m_S^* , T_{D_S} , g_S , and ϕ_S as adjustable parameters. The resulting parameters giving a best description of the data obtained by this procedure are shown in Table I. While the low-field data (< 2 T) can be adequately described by holes with low effective mass, the high-field data (> 2 T) indicate carriers with a much heavier mass ($0.075m_0$). Also shown in Fig. 6 are the results of fitting the data to a two-component synthesis. The figure shows that the component that dominates at large B is

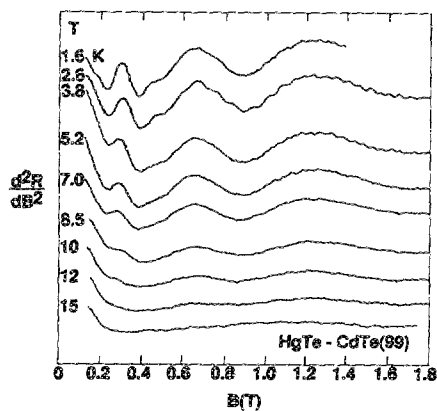


FIG. 4. Temperature dependence of the SdH oscillations in p -type sample No. 99 obtained in the low magnetic field region. The fact that the oscillations have disappeared at 15 K at these low fields indicates a low effective mass for the holes.

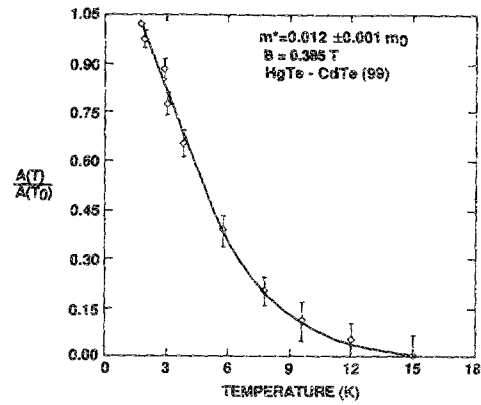


FIG. 5. Normalized SdH amplitudes as a function of temperature for sample No. 99 at low fields. The solid line shows the theoretical variation predicted from Eq. (2) using only the first harmonic SdH term with $m^* = 0.012m_0$.

nearly absent at small B . Although this would occur if the high-field component had a very high Dingle temperature ($T_D \approx 28$ K), the high T_D in conjunction with the heavy mass would also make the amplitude of the high-field oscillations too small to be observable. We therefore conclude that the differing behaviors at low and high B cannot be explained by assuming the simultaneous presence of two hole species with different masses. The data imply instead that the heavy mass carrier that dominates at high magnetic fields is not present at low fields.

We now show that such a result is actually expected on the basis of theoretical band-structure considerations. If the tight-binding calculation is applied to the well and barrier thicknesses appropriate for p -type sample Nos. 99 and 107, both superlattices are predicted to have zero band gap.¹¹ A typical band structure⁴ for this case is reproduced in Fig. 7. When E_g is near zero, the in-plane hole mass at small k_x (see the dashed curves in the figure) becomes quite small

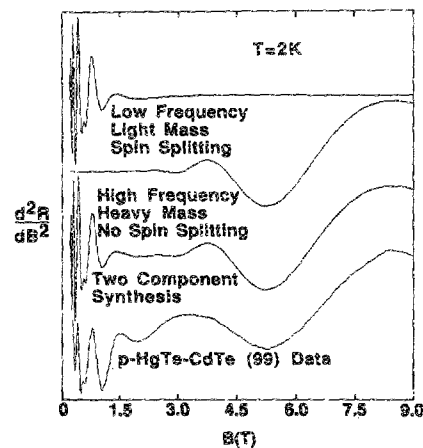


FIG. 6. Complex SdH oscillatory data measured on p -type sample No. 99 along with a theoretical synthesis from two component sets of holes. Only relative amplitudes are shown; the actual SdH amplitude of the heavy mass component is several orders of magnitude smaller than the light mass component amplitude. Thus, a remarkable similarity can be obtained for the parameters shown in Table I, but only if the heavy mass component amplitude is artificially increased by several orders of magnitude in order to accomplish the two component synthesis shown.

TABLE I. Summary of HgTe-CdTe superlattice properties determined by the SdH effect.

Sample	SdH period (kG) ⁻¹	2D concentration (cm ⁻²)	Effective mass (m ₀)	Dingle temperature (K)	Mobility at 4.2 K (cm ² /V s)	g factor	Phase factor
<i>p</i> -HgTe-CdTe(99) 70 layers HgTe(57 Å)CdTe(19 Å)							
Light mass, low-field component	0.115	4.2 × 10 ¹⁰	0.012	5.0	1.4 × 10 ⁴	64	-π/4
Heavy mass, high-field component	0.016	3.0 × 10 ¹¹	0.075	28.0	0.27 × 10 ⁴	...	π/2
<i>p</i> -HgTe-CdTe(107) 100 layers HgTe(84 Å)CdTe(37 Å)	0.14	3.5 × 10 ¹⁰	0.009
<i>n</i> -HgTe-CdTe(203) 65 layers HgTe(200 Å)CdTe(35 Å)	0.090	5.4 × 10 ¹⁰	0.021	11.0	6.3 × 10 ⁴	30	-π/4
<i>n</i> -HgTe-CdTe(204) 75 layers HgTe(54 Å)CdTe(50 Å)	none seen	≈ 10 ⁴
<i>p</i> -HgTe-CdTe(133) 75 layers HgTe(43 Å)CdTe(61 Å)	none seen	0.24 × 10 ³

(< 0.02). However, with increasing k_x the valence band dispersion becomes extremely nonparabolic. The theory predicts that for k_x greater than ≈ 0.01 , the valence-band mass becomes quite heavy, or even electronlike. Here k_x is expressed in units of $2\pi/a$, where a is the lattice constant. It is well known that there is a correspondence between Landau-level spacings as a function of magnetic field and dispersion as a function of wave vector. Neglecting spin, the relation is roughly

$$k_x \leftrightarrow [2eB(n + \frac{1}{2})/\hbar c]^{1/2},$$

where n is the Landau level number. We find that for low n one expects an abrupt increase in the hole effective mass precisely in the region where the SdH behavior changes experimentally, i.e., $B \approx 2$ T. Besides explaining our data for sample No. 99, the strong dependence of the hole effective mass on magnetic field also clarifies the apparent contradiction between the results of previous SdH studies on *p*-type HgTe-CdTe superlattices. From the SdH data for $B \leq 1.4$ T, Goodwin *et al.*² obtained a mass of $0.012m_0$, which is in good agreement with the present low-field results. On the other hand, Woo and co-workers⁶ derived a mass of $0.3m_0$ from SdH oscillations in a high-mobility *p*-type sample at much higher magnetic fields (3–8 T). Without the use of the sensitive ac magnetic field modulation technique, Woo and co-workers⁶ could not observe SdH oscillations at low B . Thus, the results of the two previous studies are not necessarily

contradictory. As verified by the data for sample No. 99, one expects a small mass at low B but a much larger mass at high B (this possibility was noted by Woo and co-workers). Similarly, it has recently been observed¹² that cyclotron resonance transitions, corresponding to holes with very light mass in *p*-type HgTe-CdTe superlattices, disappear at high B . In their place, a line corresponding to the presence of heavy electrons appears at fields above ≈ 5 T.

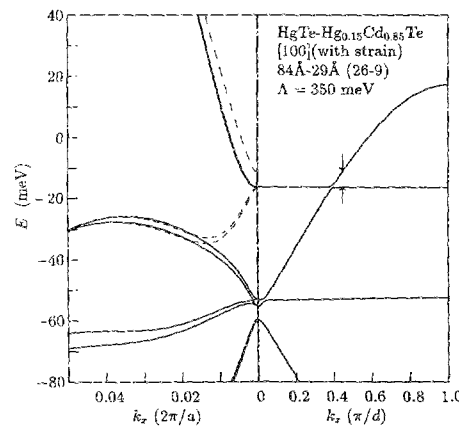


FIG. 7. Superlattice in-plane (k_x) and growth-direction (k_z) dispersion relations for $d_w = 84$ Å and $d_B = 29$ Å at $T = 0$ K. The dashed curves show the parallel electron and hole dispersion behavior for $k_z = 0.45\pi/d$ rather than $k_z = 0$, as indicated by the arrows (reproduced from Ref. 4).

We saw above that the experimental data for *n*-type sample No. 203 could be straightforwardly treated using conventional SdH analysis, giving an electron mass that compares favorably with band-structure theory. However, the analysis for narrow- and zero-gap *p*-type samples is much more difficult due to the unusual properties of the valence band. As can be seen in Fig. 7, an anticrossing of the E1 band (which has strong k_z dispersion) and the HH1 band (which is almost dispersionless) at some k_z^c leads to an indirect band alignment. Although the band gap is predicted to be less than 0.1 meV, the conduction-band minimum extends between $0 < k_z < k_z^c$ while the valence-band maximum spans the range $k_z^c < k_z < \pi/d$. Furthermore, the in-plane hole effective mass is predicted to vary between $m^* \approx 0.001m_0$ near $k_z \approx k_z^c$ and $\approx 0.02m_0$ near $k_z = \pi/d$. Because of this severe mass broadening (by a factor of ≈ 20), conventional SdH analysis is inapplicable and a new theory will be required before a detailed interpretation of the *p*-type data can be carried out.

Although we cannot perform a detailed quantitative analysis for *p*-type samples, the present results clearly show the in-plane hole effective mass to be small at low magnetic fields. It has recently been pointed out¹³ that this implies a valence-band offset of at least 200 meV. When a small offset is assumed (e.g., 40 meV), strain causes LH1 (which has heavy in-plane dispersion) to be the uppermost valence band. The resulting band structure with a heavy in-plane hole mass would be in contradiction with not only the present data, but also with the results of recent magnetotransport^{3,4} and magneto-optical studies.¹²

In summary, carrier effective masses have been determined for both *n*- and *p*-type HgTe-CdTe superlattices using the Shubnikov-de Haas effect. The electron and hole masses

found are in agreement with predictions of band-structure theory.

ACKNOWLEDGMENT

The authors thank Joel Schulman for allowing the use of his tight-binding superlattice band-structure software.

¹J. Reno, I. K. Sou, J. P. Faurie, J. M. Berroir, and Y. Guldner, *J. Vac. Sci. Technol. A* **5**, 3107 (1987).

²M. W. Goodwin, M. A. Kinch, R. J. Koestner, M. C. Chen, D. G. Seiler, and R. J. Justice, *J. Vac. Sci. Technol. A* **5**, 3110 (1987).

³J. R. Meyer, C. A. Hoffman, F. J. Bartoli, J. W. Han, J. W. Cook, Jr., J. F. Schetzina, X. Chu, J. P. Faurie, and J. N. Schulman, *Phys. Rev. B* **38**, 2204 (1988).

⁴C. A. Hoffman, J. R. Meyer, F. J. Bartoli, J. W. Han, J. W. Cook, Jr., J. F. Schetzina, and J. N. Schulman, *Phys. Rev. B* **39**, 5208 (1989).

⁵For a comprehensive review of past SdH work on a wide variety of semiconductors see D. G. Seiler, in *The Shubnikov-de Haas Effect in Semiconductors: A Comprehensive Review of Experimental Results*, edited by G. Landwehr and E. I. Rashba, to be published in *Modern Problems in Condensed Matter Science: Landau Level Spectroscopy*.

⁶K. C. Woo, S. Rafol, and J. P. Faurie, *Phys. Rev. B* **34**, 5996 (1986).

⁷N. P. Ong, J. K. Moyle, J. Bajaj, and J. T. Cheung, *J. Vac. Sci. Technol. A* **5**, 3079 (1987).

⁸L. Ghenim, R. G. Mani, J. R. Anderson, and J. T. Cheung, *Phys. Rev. B* **39**, 1419 (1989).

⁹J. N. Schulman and Y.-C. Chang, *Phys. Rev. B* **33**, 2594 (1986).

¹⁰We have taken the valence-band offset to be 350 meV and have assumed the barriers to contain 15% HgTe.

¹¹From the experimental intrinsic carrier density data discussed in Ref. 2, gaps of 30 and 3 meV were obtained for sample Nos. 99 and 107, respectively. The discussion of the SdH effect in these samples is equally appropriate for either zero or small positive band gaps.

¹²J. M. Perez, R. J. Wagner, J. R. Meyer, J. W. Han, J. W. Cook, Jr., and J. F. Schetzina, *Phys. Rev. Lett.* **61**, 2261 (1988).

¹³J. R. Meyer, F. J. Bartoli, C. A. Hoffman, and J. N. Schulman, *Phys. Rev. B* **38**, 12 457 (1988).